

Fluorescence

Photoactivatable Aggregation-Induced Emission Fluorophores with Multiple-Color Fluorescence and Wavelength-Selective Activation

Lu Peng, Yue Zheng, Xiaoyan Wang, Aijun Tong, and Yu Xiang*^[a]

Abstract: Photoactivatable (caged) fluorophores are widely used in chemistry, materials, and biology. However, the development of such molecules exhibiting photoactivatable solid-state fluorescence is still challenging due to the aggregation-caused quenching (ACQ) effect of most fluorophores in their aggregate or solid states. In this work, we developed caged salicylaldehyde hydrazone derivatives, which are of aggregation-induced emission (AIE) characteristics upon

light irradiation, as efficient photoactivatable solid-state fluorophores. These compounds displayed multiple-color emissions and ratiometric (photochromic) fluorescence switches upon wavelength-selective photoactivation, and were successfully applied for photopatterning and photoactivatable cell imaging in a multiple-color and stepwise manner.

Introduction

Photoactivatable (or caged) fluorophores^[1] are molecules showing fluorescence switches upon light irradiation, which are widely used as functional groups and probes in chemistry,^[2] materials,^[3] and biology.^[4] Unfortunately, most fluorophores, such as conventional fluorescein or rhodamine dyes, undergo aggregation-caused quenching (ACQ),^[5] which makes the activated fluorescence of their photoactivatable derivatives usually much weaker in aggregate or solid states compared to that in solutions. Organic compounds with strong solid-state fluorescence are attractive materials suitable for the fabrication of luminescent materials and many other real world applications where molecules tightly packed as aggregates or even solids are required.^[6] However, fluorophores exhibiting both photoactivatable characteristics and strong solid-state fluorescence without ACQ upon light irradiation are still much less investigated, despite of their potential applications as functional solid materials for photopatterning,^[7] photoactivatable imaging,^[8] etc.

Unlike many fluorescent dyes showing little or very weak solid-state fluorescence due to the ACQ effect, fluorophores with aggregation-induced emission (AIE) properties are an emerging class of molecules displaying strong fluorescence in their aggregate or solid states.^[9] So far, many AIE fluorophore systems^[9d] made of hydrocarbons, heteroatoms or organometallics have been characterized and developed as fluorescent

materials for applications,^[10] such as luminescent probes,^[9c,11] imaging reagents,^[9c,12] optoelectronic devices,^[13] and stimuli-responsive materials.^[9b,14] These AIE fluorophores usually exhibit a large Stokes' shift with almost no overlap between their excitation and emission spectra, so that little ACQ effect is present even when the molecules are closely packed in their aggregate or solid states. In addition, they are normally non-fluorescent in solutions because of the intramolecular motions that cause non-radiative decay of the excited states, while this process is restricted in aggregates or solids to maintain strong fluorescence.^[9d,15]

Therefore, AIE fluorophores can be an ideal platform for the development of photoactivatable solid-state fluorescent materials. By attaching a 2-nitrobenzyl group as a quencher to an AIE-active tetraphenylethene molecule, Tang and co-workers have constructed a caged fluorophore that displays a strong cyan emission with high fluorescence quantum yields in its aggregate or solid states upon UV irradiation, and applied the compound as a solid material for photopatterning and anti-counterfeiting.^[7a] Nevertheless, it is still very challenging to develop caged solid-state fluorophores with photoactivatable fluorescence in multiple colors (including ratiometric fluorescence switches) by wavelength-selective photoactivation, as well as to apply them in biological systems.

In this work, we developed a series of salicylaldehyde hydrazone derivatives,^[16] which are caged by 2-nitrobenzyl, phenacyl, or 7-methoxycoumarin-4-yl, to serve as photoactivatable solid-state fluorophores with multiple fluorescence colors upon wavelength-selective activation (Figure 1). The emission colors of these compounds upon UV irradiation were tunable from green to orange by changing the substitutions on the salicylaldehyde hydrazone,^[16] while the photoactivation of the fluorophores was selectively carried out by UV irradiation at 365 or 300 nm through varying the caging groups.^[17] Interest-

[a] L. Peng, Y. Zheng, X. Wang, Prof. A. Tong, Prof. Y. Xiang
Department of Chemistry, Beijing Key Laboratory for Analytical Methods and Instrumentation, Key Laboratory of Bioorganic Phosphorus Chemistry and Chemical Biology, Tsinghua University, Beijing 100084 (PR China)
E-mail: xiang-yu@tsinghua.edu.cn

Supporting information for this article is available on the WWW under <http://dx.doi.org/10.1002/chem.201406026>.

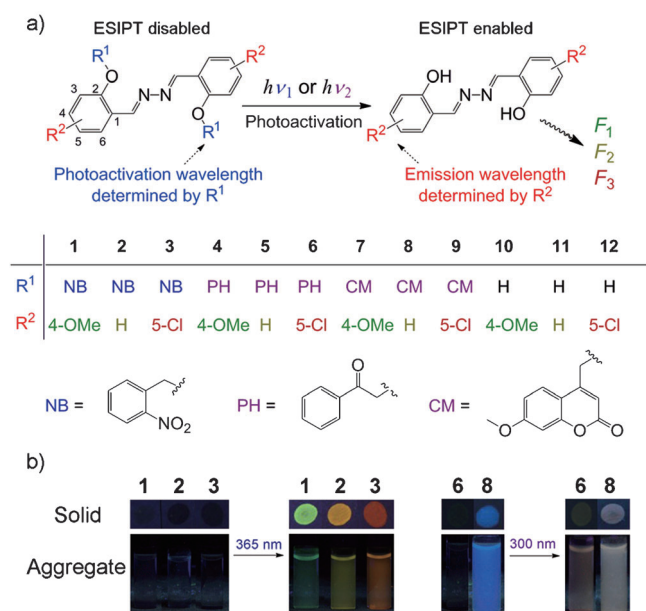


Figure 1. a) Chemical structures of compounds 1–12 and the scheme of photouncaging 1–9 to yield 10–12, which are fluorescent at different wavelengths (colors) by UV irradiation at different wavelengths. ESIPT, excited-state intramolecular proton transfer; NB, 2-nitrobenzyl; PH, phenacyl; CM, 7-methoxycoumarin-4-yl. b) The multiple-color fluorescence enhancement or change upon irradiation at 365 or 300 nm for 1 (green), 2 (yellow), 3 (orange), 6 (light orange), and 8 (from blue to white purple) in their solid and aggregate (colloid solution) states.

ingly, a ratiometric (photochromic) fluorescence switch upon UV irradiation was also achieved when using a fluorescent coumarin derivative as the caging group. Furthermore, these photoactivatable solid-state fluorophores were successfully applied for photopatterning and photoactivatable cell imaging, in a multiple-color and stepwise manner.

Results and Discussion

Design of the photoactivatable AIE fluorophores

One class of AIE-active fluorophores is based on the excited-state intramolecular proton transfer (ESIPT) mechanism,^[18] in which the hydroxyl groups of these fluorophores are responsible for ESIPT and essential for their AIE characteristics as well as solid-state fluorescence.^[9d, 16a, 19] Therefore, we expect that the solid-state fluorescence

of salicylaldehyde hydrazones, which are AIE-active by ESIPT, can be quenched by caging the hydroxyl groups and subsequently activated by uncaging through UV irradiation. As shown in Figure 1a, no ESIPT is possible in the presence of caging groups on the salicylaldehyde hydrazones 1–9 due to the absence of hydroxyl protons, thus these caged compounds should be non-fluorescent. Upon UV irradiation to remove the caging groups and yield 10–12, the hydroxyl and ESIPT can be recovered to restore the AIE and strong solid-state fluorescence. In addition to the capability of realizing multiple-color emissions upon UV irradiation by changing the substitutions on the salicylaldehyde hydrazone,^[9d, 16a, 19] another advantage of this design principle over previous reports is that the caging groups may not necessarily be quenchers,^[7a, 8, 20] so that the choice of caging groups is very flexible to enable wavelength-selective photoactivation^[3b] as well as ratiometric (photochromic) fluorescence switches upon UV irradiation.

Caged fluorophores with multiple-color photoactivatable fluorescence

The photoactivatable fluorescence of 2-nitrobenzyl-caged^[17b, 21] salicylaldehyde hydrazones 1–3 were studied first to testify our design principle (Figure 2a). All these caged compounds displayed little fluorescence in their aggregate (colloid solution, Figure S1 in the Supporting Information) or solid states, which suggests the successful caging effect of 2-nitrobenzyl; while

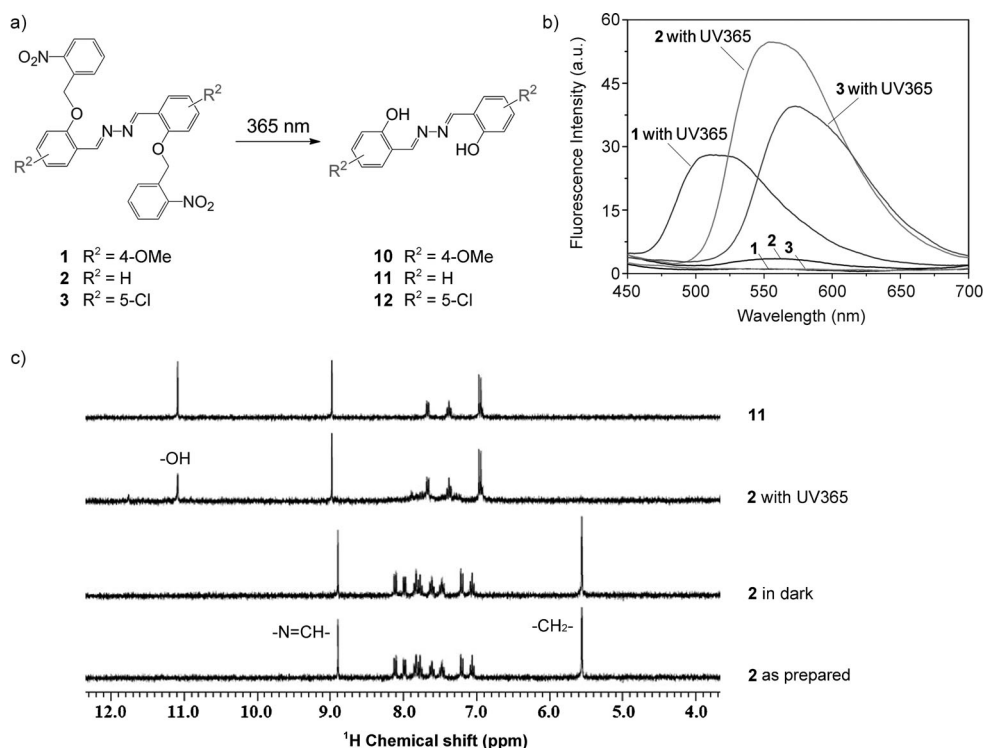


Figure 2. a) The transformation of 2-nitrobenzyl-caged salicylaldehyde hydrazones 1–3 by UV irradiation at 365 nm. b) Fluorescence spectra of 1–3 in aggregate states before and after UV irradiation at 365 nm. c) Partial ¹H NMR spectra (1 mM solutions in [D₂]DMSO) of 2 as prepared, 2 after irradiation at 365 nm, 2 after standing in the dark, and 11, which suggests the complete transformation of 2 to 11 by the UV irradiation.

upon continuous irradiation under a 12 W 365 nm handheld UV lamp, 1–3 underwent a gradual fluorescence enhancement over time until strong emissions in green (521 nm), yellow (541 nm), and orange (566 nm) were observed for 1, 2, and 3, respectively, in both of their aggregate and solid states (Figure 1b). The time-dependent fluorescence spectra of 1–3 in the colloid solutions were recorded in the absence and presence of UV irradiation at 365 nm (Figure S2–S4 in the Supporting Information), showing that the photoactivation only occurred under UV light and could be fully accomplished. Figure 2b illustrates the fluorescence spectra of 1–3 in their aggregated states before and after the irradiation, in which the fluorescence of 1–3 after the irradiation was almost identical to that of 10–12 in the same solvent (Figure S5, Supporting Information), which supports the hypothesis in our design. The photoactivatable fluorescence of 1–3 was also studied in their solid states (on a solid support for solid-state fluorescence measurement). Only background fluorescence of the solid support was observed for 1–3 without UV irradiation, regardless of the time for standing in the dark. However, upon irradiation at 365 nm, the solids of 1–3 displayed similar fluorescence emissions as those in the colloid solutions and the fluorescence gradually enhanced over time (Figure S6–S9, Supporting Information). These results demonstrated the usefulness of 1–3 as photoactivatable fluorescent materials in both colloid solutions and solids with multiple-color fluorescence emissions upon light irradiation. The photophysical properties of 1–3 are listed in Table S1 (Supporting Information).

To investigate the fate of the caged fluorophores after photoactivation, we further studied the ^1H NMR spectra of 2 in $[\text{D}_6]\text{DMSO}$ before and after the UV irradiation. As shown in Figure 2c, 2 exhibited two sharp peaks around $\delta=5.6$ and 8.9 ppm, corresponding to the signals of the CH_2 (connecting salicylaldehyde hydrazone and nitrobenzyl groups) and the $\text{N}=\text{CH}$ (salicylaldehyde hydrazone). There was no change in the ^1H NMR spectrum of 2 after standing in the dark for 1 h, which indicated the compound was stable in DMSO in the absence of UV light. Nevertheless, when 2 was irradiated at 365 nm for 1 h, the chemical shifts of the CH_2 and $\text{N}=\text{CH}$ underwent disappearance and 0.1 ppm downfield shift, respectively, while a new peak at around 11.1 ppm (OH) emerged. This spectrum of 2 after the irradiation was very similar to that of 11 (five characteristic peaks around $\delta=6.9, 7.4, 7.7, 9.0,$ and 11.1 ppm), with some minor peaks most likely ascribed to some by-products from the released 2-nitrobenzyl moiety. Therefore,

the result strongly supported the formation of 11 from 2 (Figure 2a), including the removal of the 2-nitrobenzyl and the recovery of the hydroxyl group, by UV irradiation.

Wavelength-selective photoactivation and ratiometric (photochromic) fluorescence switch

Due to the caging groups in our photoactivatable system are not necessarily quenchers, it is then possible for us to use other photosensitive groups other than 2-nitrobenzyl to construct caged solid-state fluorophores exhibiting wavelength-selective photoactivation. As depicted in Figure 3a, phenacyl-

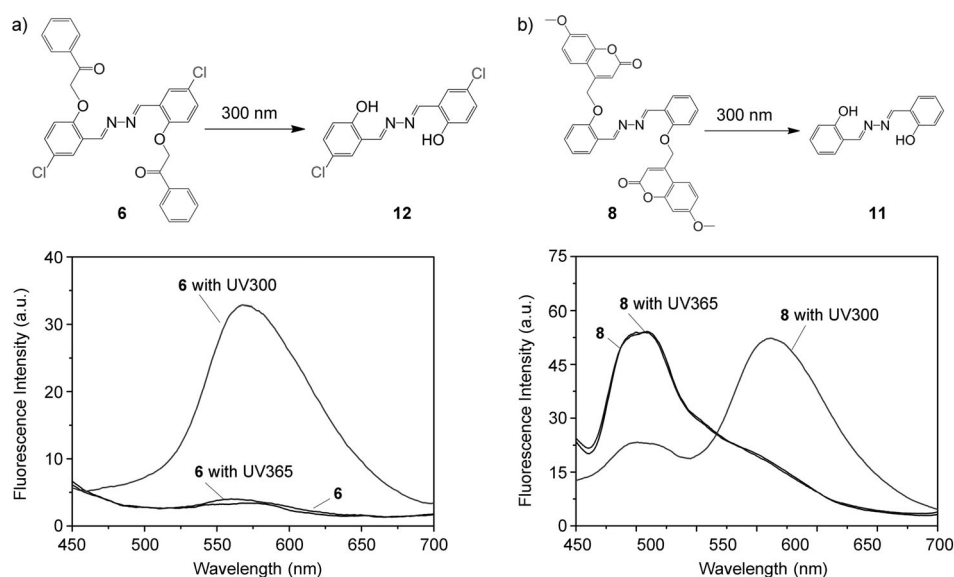


Figure 3. The transformation of a) 6 to 12 and b) 8 to 11 by UV irradiation selectively at 300 nm, and the fluorescence spectra of 6 and 8 before and after UV irradiation at 300 or 365 nm.

caged^[17b,22] salicylaldehyde hydrazones 6 showed little fluorescence in the dark or after prolonged irradiation at $\lambda=365$ nm in its aggregate or solid states, whereas the light-orange fluorescence was gradually lighted up when the irradiation was at $\lambda=300$ nm (Figure 1b), which is close to the optimal wavelength capable of removing the phenacyl group^[17b,22] from non-fluorescent 6 to yield fluorescent 12. The kinetics of the fluorescence enhancement upon 300 nm irradiation was monitored (Figure S10, Supporting Information), which was slower compared to those of 1–3 (Figure S2–S4, Supporting Information) due to the lower quantum efficiency of phenacyl versus that of 2-nitrobenzyl.^[17b,22] The time-dependent solid-state fluorescence spectra of 4–6 after standing in dark or irradiated by $\lambda=365$ or 300 nm UV light were also studied. They were all found to display photoactivated fluorescence enhancement over the background only in the presence of 300 nm irradiation, while almost no change occurred in the dark or under irradiation at 365 nm (Figure S11–S13, Supporting Information), thereby enabling multiple wavelength-selective photoactivation.

More interestingly, when we utilized 7-methoxycoumarin-4-yl^[17b,23] as a caging group that was fluorescent itself, the fluorophores **8** exhibited a ratiometric (photochromic) fluorescence switch instead of solely photoactivation after UV irradiation. As shown in Figure 3b, **8** displayed blue fluorescence in its aggregate or solid states because of the weakly fluorescent coumarin as a caging group (significantly quenched compared to its fluorescence in solution, as displayed in Figure S14 Supporting Information). Upon light irradiation at 300 nm, the coumarin should be removed from **8** and the resulting compounds exhibited combined fluorescence characteristics of both 7-methoxycoumarin (blue) and salicylaldehyde hydrazones **11** (yellow), which appeared as fluorescence in white purple (Figure 1b). This photochromic fluorescence was only observed after 300 nm irradiation, not in dark or under 365 nm light (Figure S15, Supporting Information), because the caging group's photosensitive wavelength is close to 300 nm.^[17b,23] The solids of 7–9 were also measured on the solid support to investigate their photoactivatable fluorescence properties, and they were all found to undergo similar fluorescence switches solely upon irradiation at 300 nm (Figure S16–S19, Supporting Information). The photophysical properties of 4–9 are also listed in Table S1 (Supporting Information).

Multiple-color and stepwise photopatterning

Encouraged by the above results showing the efficient photoactivatable fluorescence of our caged salicylaldehyde hydrazones in solid states, we further applied these molecules as materials for photopatterning^[7] in a multiple-color and stepwise manner. As displayed in Figure 4a, upon light irradiation

at 365 nm through a photomask, the words "CHEMISTRY" fluorescent in green, yellow and orange were successfully patterned on filter papers preloaded loaded with solids of **1**, **2** and **3**, respectively, whereas the use of **8** enabled the patterning of a fluorescent "CHEMISTRY" in white purple on a blue background after UV irradiation at 300 nm. By drawing an image of flowers and leaves using **1–3** as the "dyes" on the same paper (Figure 4b), the initially invisible image containing three colors showed up when the paper was irradiated under $\lambda = 365$ nm UV light, which indicated the success of multiple-color photopatterning in one image. More interesting, if some of the flowers in the image were drawn using **8** instead of **2**, the photopatterning could be carried out in not only a multiple-color fashion but also a stepwise manner by sequential light irradiations at $\lambda = 365$ and 300 nm (Figure 4c). At first, the image was only visible as two blue flowers. Subsequently, orange flowers and green leaves emerged upon light irradiation at 365 nm. Further, the blue flowers turned white purple as the light irradiation was altered to 300 nm.

Photoactivatable cell imaging

In addition to the application of the caged salicylaldehyde hydrazones in their solid states for photopatterning, we also investigated the use of these molecules in their colloid solutions (aggregate states) for photoactivatable cell imaging.^[8] The formation of colloids of **1–3** and **8** in aqueous solutions was supported by the results of dynamic light scattering (DLS) analysis (Figure S1, Supporting Information). The diameters of the particles in the colloid solutions were in the range of 130–190 nm, which is suitable for cellular uptake through endocytosis. After incubating MCF-7 cells with each of the colloid solutions of the caged fluorophores **1–3**, the cells were washed thoroughly and irradiated at $\lambda = 365$ nm or in dark for 40 min before imaged under a fluorescence microscope. As shown in Figure 5a–c, cells containing **1–3** displayed almost no detectable fluorescence under the microscope before UV irradiation or after the incubation in dark. However, upon irradiation at 365 nm, green, yellow and orange fluorescence gradually arose inside the cells with **1**, **2** and **3**, respectively (Figure 5a–c, and Figure S20–S22 in the Supporting Information). The fluorescent dots were found mostly localized in the cytoplasm of the cells rather than in the nucleus, mainly because some of the uncaged fluorophore molecules (containing phenol groups) on

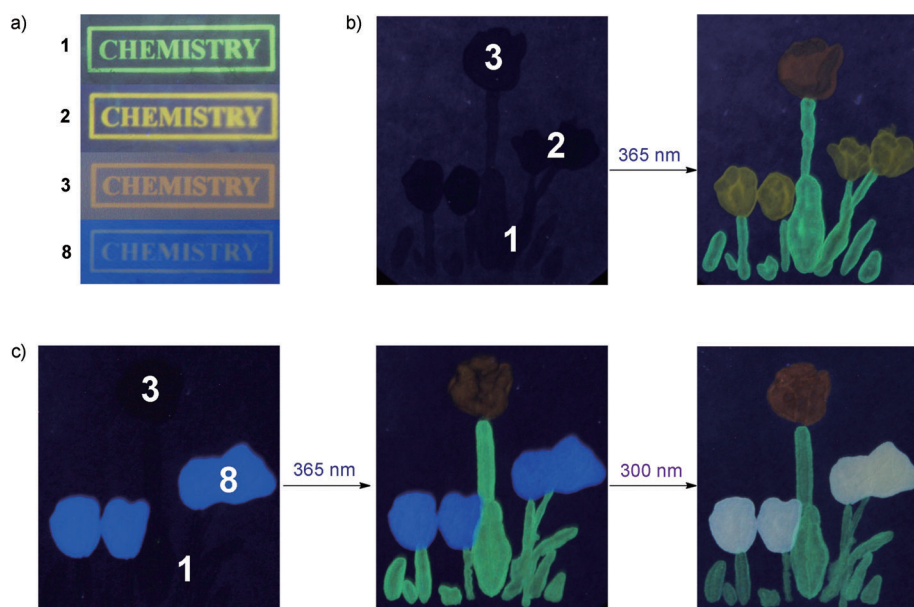


Figure 4. a) Patterning words of "CHEMISTRY" in green (**1**), yellow (**2**), orange (**3**), and white purple on a blue background (**8**) using a photomask on papers loaded with one of the photoactivatable fluorophores as solids. b) Photoactivating a multiple-color fluorescent image of flowers (orange and yellow) and leaves (green) made of **1–3** as solids by UV irradiation at 365 nm. c) Stepwise photoactivating a multiple-color fluorescent image of flowers (blue, orange and white purple) and leaves (green) made of **1**, **3** and **8** as solids by sequential UV irradiations at 365 and 300 nm.

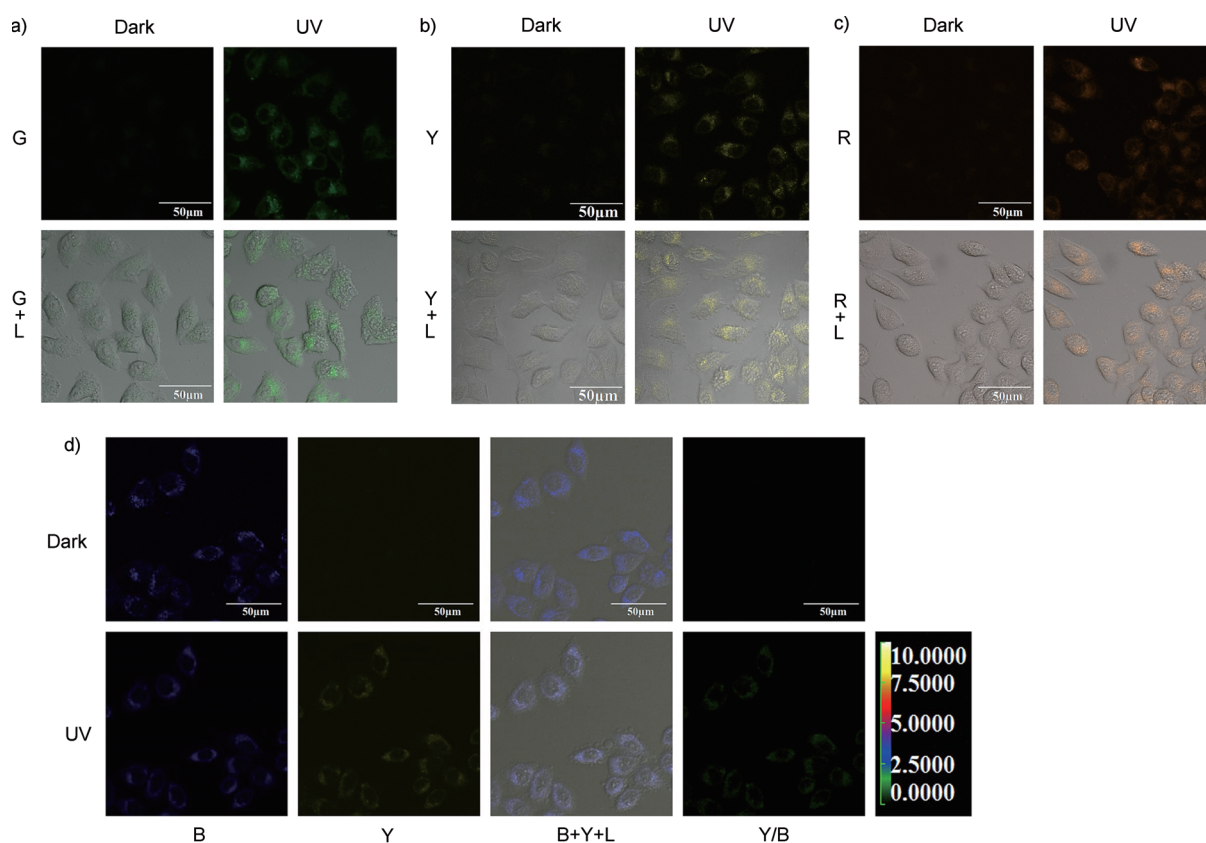


Figure 5. Fluorescent live cell images of MCF-7 cells containing a) **1**, b) **2**, or c) **3** after incubation without or with UV irradiation at 365 nm. d) Ratiometric fluorescent live cell images of MCF-7 cells containing **8** after incubation without or with UV irradiation at 300 nm. “Dark”, in dark; “UV”, with UV irradiation; “B”, “G”, “Y”, “R”, and “L”: blue, green, yellow, red, and bright channels, respectively; “Y/B”, intensity ratio of yellow channel divided by blue channel.

the surface of the particles might undergo ionization to generate negative charges. On the other hand, cells incubated with **8** were found to exhibit ratiometric fluorescence switches after UV irradiation at 300 nm (Figure 5d, and Figures S23–S24 in the Supporting Information), as illustrated in the images using color scales of intensity ratio (yellow channel divided by blue channel). Ratiometric fluorescence switches are usually much less susceptible to the interference from photobleaching or concentration distributions of fluorophores inside cells, compared with fluorescence enhancement alone.^[24] These results demonstrated that our caged fluorophores were successfully delivered into live cells and fully preserved their photoactivatable fluorescence in the cellular environment.

Conclusions

In summary, we have developed caged salicylaldehyde hydrazone derivatives showing photoactivatable solid-state fluorescence in this study. Upon UV irradiation, the caging groups blocking the hydroxyl moieties of these fluorophores were removed, thereby recovering ESIPT and strong fluorescence in their aggregate (colloid solution) and solid states. By changing the substitutions on the salicylaldehyde hydrazone and varying the caging groups on the hydroxyl group, photo-

activatable solid-state fluorescence of multiple emission colors and wavelength-selective activation were achieved, respectively. The use of a fluorescent caging group also enabled a ratiometric (photochromic) fluorescence switch upon UV irradiation. The caged salicylaldehyde hydrazones were further successfully applied for photopatterning and photoactivatable cell imaging in a multiple-color and stepwise manner, which suggests their promising potential as photoactivatable solid-state fluorophores in chemistry, materials, and biology.

Experimental Section

Materials and instrumentation

All chemicals were purchased either from Alfa Aesar (Tianjin, China) or Sigma–Aldrich (St. Louis, USA) and used as received without further purification. The 10 mM HEPES buffer at pH 7.0 was prepared by adding a proper amount of NaOH to HEPES in Millipore water under adjustment by a pH meter. All absorption and fluorescence spectra were measured on a JASCO V-550 spectrophotometer and a JASCO FP-6500 spectrophotometer (Tokyo, Japan). All NMR spectra were recorded using a JOEL JNM-ECA300 spectrometer (Tokyo, Japan) operated at 300 MHz. Cell imaging was performed on an Olympus FV 1000 confocal microscope (Tokyo, Japan).

Photoactivation of the fluorophores in aggregate states (colloid solutions)

Stock solutions (2.0 mM) of compounds **1–9** were prepared in DMSO. In a typical experiment, the colloid solution was prepared by placing 25 μL of the stock solution into 475 μL 10 mM HEPES at pH 7.0 with rigorous mixing. The solutions were irradiated by a 12 W hand-held UV lamp (5 cm above the solutions) at 365 or 300 nm for a desired time, then absorption and fluorescence spectra were recorded at 25 °C. Excitation was at 370 nm.

Photoactivation of the fluorophores in solid states

Stock solutions (2.0 mM) of compounds **1–9** were prepared in THF. In a typical experiment, 3 μL of each stock solution was dropped on a filter paper strip. After complete evaporation and dried, the paper strips was irradiated by a 12 W hand-held UV lamp (5 cm above the spots) at 365 or 300 nm for a desired time, then fluorescence spectra were recorded at 25 °C. Excitation was at 370 nm.

Multiple-color and stepwise photopatterning

Papers were fully soaked by stock solutions (2.0 mM) of **1**, **2**, **3** and **8** in THF, and dried under ambient condition. The photopatterning of the word "CHEMISTRY" was carried out by irradiating the papers at 365 or 300 nm for 30 min under a plastic photomask (with the "CHEMISTRY" pattern) printed by a standard printer. For images of flowers and leaves, the stock solutions were used as the "dye" for the drawings on a paper by brush pens. After having been dried under ambient conditions, the paper was irradiated at $\lambda = 365$ or 300 nm for 30 min. The visualization of the fluorescent images was through the excitation by a $\lambda = 365$ nm UV lamp for a short time (within 5 s) to minimize unwanted activation.

Photoactivatable cell imaging

MCF-7 cells were obtained from NIH (Bethesda, USA) and the reagents for culture were purchased from HyClone (Waltham, USA). The cells were planted at 1×10^5 cells mL^{-1} on non-coated glass-bottomed dishes and cultured in Dulbecco's modified Eagle medium (DMEM) containing 10% fetal bovine serum, 100 I.U. mL^{-1} penicillin and 100 $\mu\text{g mL}^{-1}$ streptomycin at 37 °C in a 5% CO_2 incubator. After 24 h of incubation in DMEM, the cells were washed twice with DMEM.

In a typical experiment, loading solutions of **1**, **2**, **3**, and **8** were prepared by placing 25 μL of their DMSO stock solutions (2.0 mM) into a microtube, and then the solutions were diluted to 1 mL with DMEM with vigorous mixing. The loading solutions containing 50 μM **1**, **2**, **3**, or **8** were added to the cells and incubated for 1 h at 37 °C. The cells were then washed with 1 mL DMEM for three times to remove free fluorophores. After incubating the cells in dark or irradiated at $\lambda = 365$ or 300 nm for a desired time, the fluorescence imaging of the cells was implemented. Excitation laser of the fluorescence microscope was at 405 nm.

General procedures for the synthesis of compound 1–9

2-Nitrobenzyl bromide (1 equiv) was dissolved in acetonitrile. Then cesium carbonate (2 equiv) and one of the salicylaldehydes (1 equiv) in acetonitrile was added. After being stirred for 3 h at room temperature, the solvent was removed under reduced pressure and the residue was extracted with CH_2Cl_2 for three times. Then the organic layer was washed with 0.2 M NaOH aqueous solu-

tion and brine, dried over anhydrous sodium sulfate, filtered and evaporated under reduced pressure. After drying, 2-nitrobenzyl-caged salicylaldehydes as precursors for the synthesis of **1–3** were obtained. One of the 2-nitrobenzyl-caged salicylaldehydes (2 equiv) was dissolved in CH_2Cl_2 or DMF, followed by the addition of hydrazine hydrate (1 equiv). After being stirred overnight at room temperature, the crude product was precipitated by adding ethanol, filtered and washed by ethanol twice to afford **1–3** after drying.

Compounds **7–9** were prepared by a similar procedure as **1–3** using 7-methoxycoumarin-4-yl bromide instead of 2-nitrobenzyl bromide. Compounds **10–12** were synthesized following the reported procedure.^[16b] Compounds **4–6** were obtained by a similar procedure as **1–3** using **10–12** and phenacyl bromide instead of salicylaldehydes and 2-nitrobenzyl bromide, respectively.

For additional figures and more details of the synthesis, see the Supporting Information.

Acknowledgements

We thank for the financial support from the National Natural Science Foundation of China (nos. 2142200199, 21390410 and 21375074), the National Key Scientific Instrument and Equipment Development Project of China (no. 2012YQ030111), the Tsinghua University Initiative Scientific Research Program (no. 20131089220), and the Recruitment Program of Global Youth Experts of China.

Keywords: aggregation-induced emission · cell imaging · fluorescence · hydrazones · photoactivatable fluorophores

- [1] T. J. Mitchison, K. E. Sawin, J. A. Theriot, K. Gee, A. Mallavarapu in *Caged Fluorescent Probes*, Vol. 291 (Ed.: M. Gerard), Academic Press, **1998**, pp. 63–78.
- [2] a) G. H. McGall, A. D. Barone, M. Diggelmann, S. P. A. Fodor, E. Gentalen, N. Ngo, *J. Am. Chem. Soc.* **1997**, *119*, 5081–5090; b) S. W. Li, D. Bowerman, N. Marthandan, S. Klyza, K. J. Luebke, H. R. Garner, T. Kodadek, *J. Am. Chem. Soc.* **2004**, *126*, 4088–4089.
- [3] a) M. Alvarez, A. Best, S. Pradhan-Kadam, K. Koynov, U. Jonas, M. Kreiter, *Adv. Mater.* **2008**, *20*, 4563–4567; b) V. San Miguel, C. G. Bochet, A. del Campo, *J. Am. Chem. Soc.* **2011**, *133*, 5380–5388.
- [4] a) H. Kobayashi, P. L. Choyke, *Acc. Chem. Res.* **2011**, *44*, 83–90; b) W. H. Li, G. H. Zheng, *Photochem. Photobiol. Sci.* **2012**, *11*, 460–471.
- [5] a) J. B. Birks, *Photophysics of Aromatic Molecules*, Wiley, New York, **1970**; b) R. B. Thompson, *Fluorescence Sensors and Biosensors*, CRC, Boca Raton, **2006**.
- [6] a) Y. Ooyama, Y. Harima, *Eur. J. Org. Chem.* **2009**, 2903–2934; b) R. P. Ortiz, J. Casado, V. Hernandez, J. T. L. Navarrete, J. A. Letizia, M. A. Ratner, A. Facchetti, T. J. Marks, *Chem. Eur. J.* **2009**, *15*, 5023–5039.
- [7] a) C. Y. Yu, R. T. K. Kwok, J. Mei, Y. N. Hong, S. J. Chen, J. W. Y. Lama, B. Z. Tang, *Chem. Commun.* **2014**, *50*, 8134–8136; b) K. Li, Y. Xiang, X. Y. Wang, J. Li, R. R. Hu, A. J. Tong, B. Z. Tang, *J. Am. Chem. Soc.* **2014**, *136*, 1643–1649.
- [8] T. Kobayashi, T. Komatsu, M. Kamiya, C. Campos, M. Gonzalez-Gaitan, T. Terai, K. Hanaoka, T. Nagano, Y. Urano, *J. Am. Chem. Soc.* **2012**, *134*, 11153–11160.
- [9] a) Y. N. Hong, J. W. Y. Lam, B. Z. Tang, *Chem. Soc. Rev.* **2011**, *40*, 5361–5388; b) Z. G. Chi, X. Q. Zhang, B. J. Xu, X. Zhou, C. P. Ma, Y. Zhang, S. W. Liu, J. R. Xu, *Chem. Soc. Rev.* **2012**, *41*, 3878–3896; c) D. Ding, K. Li, B. Liu, B. Z. Tang, *Acc. Chem. Res.* **2013**, *46*, 2441–2453; d) J. Mei, Y. N. Hong, J. W. Y. Lam, A. J. Qin, Y. H. Tang, B. Z. Tang, *Adv. Mater.* **2014**, *26*, 5429–5479.
- [10] Y. N. Hong, J. W. Y. Lam, B. Z. Tang, *Chem. Commun.* **2009**, 4332–4353.
- [11] a) M. Zhang, G. X. Feng, Z. G. Song, Y. P. Zhou, H. Y. Chao, D. Q. Yuan, T. T. Y. Tan, Z. G. Guo, Z. G. Hu, B. Z. Tang, B. Liu, D. Zhao, *J. Am. Chem.*

- Soc. **2014**, *136*, 7241–7244; b) H. B. Shi, J. Z. Liu, J. L. Geng, B. Z. Tang, B. Liu, *J. Am. Chem. Soc.* **2012**, *134*, 9569–9572; c) Z. T. Liu, W. X. Xue, Z. X. Cai, G. X. Zhang, D. Q. Zhang, *J. Mater. Chem.* **2011**, *21*, 14487–14491; d) Q. Chen, N. Bian, C. Cao, X. L. Qiu, A. D. Qi, B. H. Han, *Chem. Commun.* **2010**, 46, 4067–4069; e) L. H. Peng, M. Wang, G. X. Zhang, D. Q. Zhang, D. B. Zhu, *Org. Lett.* **2009**, *11*, 1943–1946.
- [12] a) H. B. Shi, R. T. K. Kwok, J. Z. Liu, B. G. Xing, B. Z. Tang, B. Liu, *J. Am. Chem. Soc.* **2012**, *134*, 17972–17981; b) Y. Y. Yuan, R. T. K. Kwok, B. Z. Tang, B. Liu, *J. Am. Chem. Soc.* **2014**, *136*, 2546–2554; c) K. Li, B. Liu, *Chem. Soc. Rev.* **2014**, *43*, 6570–6597.
- [13] a) Z. J. Zhao, C. M. Deng, S. M. Chen, J. W. Y. Lam, W. Qin, P. Lu, Z. M. Wang, H. S. Kwok, Y. G. Ma, H. Y. Qiu, B. Z. Tang, *Chem. Commun.* **2011**, 47, 8847–8849; b) J. Huang, R. L. Tang, T. Zhang, Q. Q. Li, G. Yu, S. Y. Xie, Y. Q. Liu, S. H. Ye, J. G. Qin, Z. Li, *Chem. Eur. J.* **2014**, *20*, 5317–5326.
- [14] a) B. J. Xu, Z. G. Chi, X. Q. Zhang, H. Y. Li, C. J. Chen, S. W. Liu, Y. Zhang, J. R. Xu, *Chem. Commun.* **2011**, 47, 11080–11082; b) Q. Lin, B. Sun, Q. P. Yang, Y. P. Fu, X. Zhu, T. B. Wei, Y. M. Zhang, *Chem. Eur. J.* **2014**, *20*, 11457–11462.
- [15] N. L. Leung, N. Xie, W. Yuan, Y. Liu, Q. Wu, Q. Peng, Q. Miao, J. W. Lam, B. Z. Tang, *Chem. Eur. J.* **2014**, *20*, 15349–15353.
- [16] a) M. Gao, Q. Hu, G. Feng, B. Z. Tang, B. Liu, *J. Mater. Chem. B* **2014**, *2*, 3438–3442; b) W. X. Tang, Y. Xiang, A. J. Tong, *J. Org. Chem.* **2009**, *74*, 2163–2166.
- [17] a) C. G. Bochet, *Angew. Chem. Int. Ed.* **2001**, *40*, 2071–2073; *Angew. Chem.* **2001**, *113*, 2140–2142; b) P. Klan, T. Solomek, C. G. Bochet, A. Blanc, R. Givens, M. Rubina, V. Popik, A. Kostikov, J. Wirz, *Chem. Rev.* **2013**, *113*, 119–191.
- [18] a) S. Lochbrunner, T. Schultz, M. Schmitt, J. P. Shaffer, M. Z. Zgierski, A. Stolow, *J. Chem. Phys.* **2001**, *114*, 2519–2522; b) T. Mutai, H. Sawatani, T. Shida, H. Shono, K. Araki, *J. Org. Chem.* **2013**, *78*, 2482–2489.
- [19] R. R. Wei, P. S. Song, A. J. Tong, *J. Phys. Chem. C* **2013**, *117*, 3467–3474.
- [20] T. Kobayashi, Y. Urano, M. Kamiya, T. Ueno, H. Kojima, T. Nagano, *J. Am. Chem. Soc.* **2007**, *129*, 6696–6697.
- [21] a) A. Patchornik, B. Amit, R. B. Woodward, *J. Am. Chem. Soc.* **1970**, *92*, 6333–6335; b) S. Laimgruber, W. J. Schreier, T. Schrader, F. Koller, W. Zinth, P. Gilch, *Angew. Chem. Int. Ed.* **2005**, *44*, 7901–7904; *Angew. Chem.* **2005**, *117*, 8114–8118.
- [22] a) A. Banerjee, D. E. Falvey, *J. Am. Chem. Soc.* **1998**, *120*, 2965–2966; b) J. Literak, A. Dostalova, P. Klan, *J. Org. Chem.* **2006**, *71*, 713–723.
- [23] a) R. S. Givens, B. Matuszewski, *J. Am. Chem. Soc.* **1984**, *106*, 6860–6861; b) R. S. Givens, M. Rubina, J. Wirz, *Photochem. Photobiol. Sci.* **2012**, *11*, 472–488.
- [24] Z. Song, R. T. Kwok, E. Zhao, Z. He, Y. Hong, J. W. Lam, B. Liu, B. Z. Tang, *ACS Appl. Mater. Interfaces* **2014**, *6*, 17245–17254.

Received: November 8, 2014

Published online on ■ ■ ■, 0000

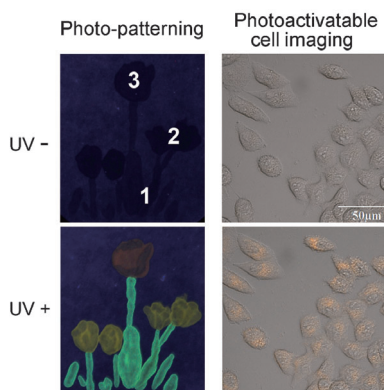
FULL PAPER

Fluorescence

L. Peng, Y. Zheng, X. Wang, A. Tong,
Y. Xiang*



 **Photoactivatable Aggregation-Induced Emission Fluorophores with Multiple-Color Fluorescence and Wavelength-Selective Activation**



Get photoactive: Photoactivatable aggregation-induced emission (AIE) fluorophores based on caged salicylaldehyde hydrazone derivatives display strong solid-state fluorescence upon UV irradiation, and are successfully applied for photopatterning and photoactivatable cell imaging in a multiple-color and stepwise manner (see figure).